Ferromagnetic resonance in magnetic multilayer structures

S. W. McKnight and C. Vittoria
Center for Electromagnetics Research, Department of Electrical and Computer Engineering, Northeastern University, Boston, Massachusetts 02192
(Received 17 April 1987)

We have calculated the FMR line shape for magnetic multilayer structures of alternating iron and iron-alloy layers. The model assumes abrupt interfaces and that spins on adjacent layers are ferromagnetically coupled with an exchange constant A_{12}. The surface magnetic anisotropy fields are set to zero in our calculations. As A_{12} is increased, satellite lines in the surface impedance split off from the ferromagnetic resonance main lines of the component materials. The number of satellites is one more than the number of layered pairs. The position and strength of these lines is found to be dependent on the relative layer thicknesses as well as the interlayer exchange coupling.

INTRODUCTION

The microwave properties of magnetic multilayer structures have been the subject of much current interest,[1-8] both because of the possibility of practical devices and structures, and because of what the properties of these structures can reveal about basic magnetic phenomena. The interaction between layers of different magnetic materials is determined by both the macroscopic dipole interaction between layers and the microscopic exchange interactions between dissimilar atoms. Of these two effects the determination of the exchange interaction is of more fundamental interest. In this paper we will present a calculation of the microwave ferromagnetic resonance (FMR) line shape in a magnetic multilayer structure where alternate layers of two different magnetic materials are coupled by the microscopic exchange interaction between the different atoms. We will assume the incident radiation and the static applied field are along the z direction and perpendicular to the layers which extend to infinity in the x and y directions. In this geometry, the dipole fields modify the internal static fields by the demagnetization effect, but the transverse rf fields do not couple by the dipole interaction since the relevant surface poles are located at infinity. This geometry is approximated by thin layered structures. We find that the FMR line shape is strongly influenced by the interlayer exchange coupling. In particular we find that increasing the interlayer exchange coupling creates satellite peaks that split off of the FMR resonances of the component materials. The total number of FMR peaks is found equal to one more than the number of layer pairs. The size of the splitting of these satellite lines and their dependence on film thickness is a sensitive function of the interlayer exchange coupling which can be related to the microscopic exchange interaction.

METHOD OF ANALYSIS

We begin by considering the layered structure indicated in Fig. 1 composed of $2N+1$ alternate layers of ferromagnetic materials A and B (with parameters chosen to represent iron and an iron alloy), where N is the number of pair layers. The layers extend to infinity in the x-y plane and the interfaces are assumed to be abrupt. There is a static external magnetic field in the z direction and both materials have their static magnetization along the external field. Identical microwave excitations are normally incident on the structure from the $+z$ and $-z$ directions. The internal microwave electric and magnetic fields in each layer are denoted by e_i and h_i. Because of the interaction with the spin-wave modes, inside the magnetic layers there are four[9] allowable circularly polarized propagating electromagnetic modes, each with its own complex propagation vector k. The k vectors for these modes can be found at each value of the internal static magnetic field by numerically solving the relevant dispersion relations, as shown in Fig. 2. Two of the four values of k correspond to magnetic resonance modes and the other two to antiresonant modes. In this paper only the two resonant modes are of interest, since we are calculating FMR line shapes of layered structures. We therefore take only the active polarization modes for each direction of propagation. This means that the microwave properties are reciprocal with respect to the direction of the incident electromagnetic wave. In an ordinary dielectric medium there is only one allowable propagation constant. However, if we include magnetoelastic motion, there are seven normal modes.[9] Nevertheless, the procedure developed in this paper is still applicable.

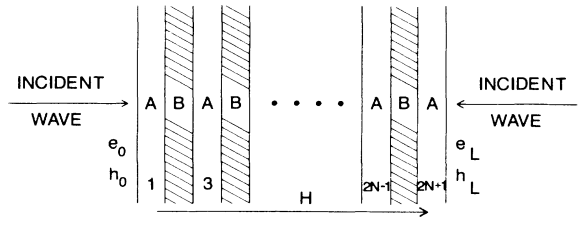

FIG. 1. Spatial configuration of layered magnetic structure. Magnetic parameters associated with layers A and B are the same as those of iron and iron alloy, respectively. The layered structure is symmetrically excited.

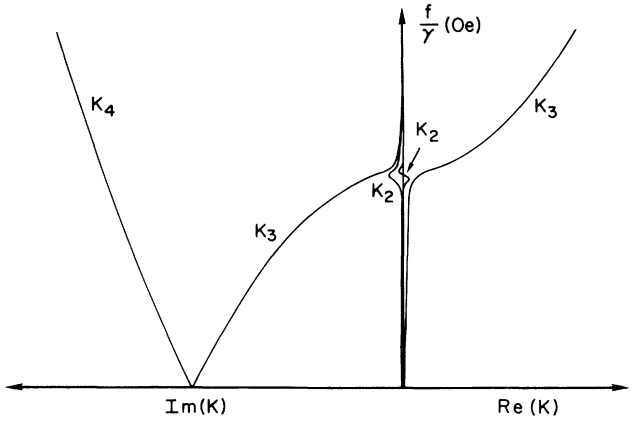

FIG. 2. Dispersion of the four propagation constants in a magnetoconductive media. Propagation constants K_2 and K_3, as displayed in this plot, correspond to the magnetically resonant modes. K_1, the electromagnetic skin depth mode, lies very close to the vertical axis.

At the interfaces, Maxwell's equations give us the condition that the tangential components of the microwave e and h fields must be continuous. We express the fields at each internal interface in terms of the component contribution from the modes propagating to the left and the right. This allows us to express the field at the second interface of that layer by multiplying by the phase factor e^{ikd}, where d is the film thickness. At the left-hand-side vacuum interface, for example, the total external field e and h is given in terms of the amplitudes of the right $(+)$ and left $(-)$ traveling waves in the first layer (circularly polarized in the magnetically active sense) as

$$h_0(z=0)=\sum_{\mu=1,2}(h_{1\mu}^{+}+h_{1\mu}^{-})\equiv h_1(z=0)\ , \tag{1a}$$

$$e_0(z=0)=\sum_{\mu=1,2}(Z_{1\mu}h_{1\mu}^{+}-Z_{1\mu}h_{1\mu}^{-})\equiv e_1(z=0)\ , \tag{1b}$$

where the sum is over the two magnetically resonant k values. The characteristic impedances $Z_{1\mu}$ can be found from the corresponding k values by $Z_{1\mu}=ick_{1\mu}/4\pi\sigma$.

At the second interface $(z=d_1)$ the field in layer 1 is given as

$$h_1(z=d_1)=\sum_{\mu}(h_{1\mu}^{+}e^{-ik_{1\mu}d_1}+h_{1\mu}^{-}e^{ik_{1\mu}d_1})\ , \tag{2a}$$

$$e_1(z=d_1)=\sum_{\mu}(Z_{1\mu}h_{1\mu}^{+}e^{-ik_{1\mu}d_1}-Z_{1\mu}h_{1\mu}^{-}e^{ik_{1\mu}d_1})\ , \tag{2b}$$

and the fields in layer 2 at the same interface $(z=d_1)$ are

$$h_2(z=d_1)=\sum_{\mu}(h_{2\mu}^{+}e^{-ik_{2\mu}d_1}+h_{2\mu}^{-}e^{ik_{2\mu}d_1})\ , \tag{3a}$$

$$e_2(z=d_1)=\sum_{\mu}(Z_{2\mu}h_{2\mu}^{+}e^{-ik_{2\mu}d_1}-Z_{2\mu}h_{2\mu}^{-}e^{ik_{2\mu}d_1})\ . \tag{3b}$$

It is noted that $k_{1\mu}\neq k_{2\mu}$, since the two adjacent layers are chosen to be magnetically different. Hence, $Z_{1\mu}\neq Z_{2\mu}$.

Setting $h_1=h_2$ and $e_1=e_2$ at $z=d_1$ gives us two equations at the interface. The continuity of e and h give two equations at each interface while we introduce four unknowns: the fields $h_{n\mu}^{\pm}$ in each layer, where n indicates the particular layer. For n odd it indicates an iron layer and n even it indicates an iron-alloy layer. Two more equations at each interface will be introduced by the spin (magnetization) boundary conditions.

SPIN BOUNDARY CONDITIONS

At a free surface it is known that the magnetization must satisfy the boundary condition

$$\frac{2A}{|\mathbf{M}|^2}\mathbf{M}\times\frac{\partial\mathbf{M}}{\partial\mathbf{q}}+\mathbf{T}_{\text{surf}}=\mathbf{0}\ , \tag{4}$$

where $\mathbf{M}$ is the total magnetization, A is the exchange stiffness constant, $\mathbf{q}$ is a coordinate vector normal to the surface, and $\mathbf{T}_{\text{surf}}$ is the torque induced by a surface magnetic anisotropy field $\mathbf{H}_s$. At an interface between two films, $\mathbf{T}_{\text{surf}}$ can also result[4] from the exchange coupling between the atoms of the two different materials. If the microscopic exchange coupling between the atoms of layer 1 and 2 is given by

$$E_s=-J_{\text{NN}}\mathbf{S}_1\cdot\mathbf{S}_2\ , \tag{5}$$

where J_{NN} is the nearest-neighbor exchange interaction parameter and $\mathbf{S}_1$ and $\mathbf{S}_2$ are the spin-moment variables at two sites each located across the interface. Using semiclassical approximations to Eq. (5), we may write

$$E_s'=-\frac{A_{12}}{M_1M_2}\mathbf{M}_1\cdot\mathbf{M}_2\ . \tag{6}$$

The prime is to denote that a molecular-field approximation has been applied to Eq. (6). A_{12} is defined in terms of J_{NN} as

$$A_{12}=\frac{J_{\text{NN}}}{a^2}\langle\mathbf{S}_1\rangle\cdot\langle\mathbf{S}_2\rangle\ . \tag{7}$$

The constant a is the distance between the two spin moments across the interface. For most cases of interest it may be taken as the lattice constant of either layer. The assumption is that both layers have the same crystal structure. The brackets represent both spin orientation and thermodynamic averages.

The surface torque due to the interlayer exchange is then

$$\mathbf{T}_{\text{surf}}=\mathbf{M}_1\times\left[-\frac{1}{M_1}\nabla E_s'\right]=\frac{A_{12}}{M_1M_2}\mathbf{M}_1\times\mathbf{M}_2\ . \tag{8}$$

The boundary condition for $\mathbf{M}_1$ is

$$\frac{A_1}{|\mathbf{M}_1|^2}\mathbf{M}_1\times\frac{\partial\mathbf{M}_1}{\partial\mathbf{q}}+\frac{A_{12}}{M_1M_2}\mathbf{M}_1\times\mathbf{M}_2+\mathbf{M}_1\times\mathbf{H}_s=\mathbf{0}\ , \tag{9}$$

and a similar equation holds for $\mathbf{M}_2$ at the interface. $\mathbf{H}_s$ may represent any other source of surface magnetic anisotropy field.[10] If we separate the magnetization into a static magnetization in the z direction and a small transverse microwave component ($\mathbf{m}$), it may be possible to linearize Eq. (9). Hence, we may write

$$A_1\frac{\partial \mathbf{m}_1}{\partial \mathbf{q}}+K_s\mathbf{m}_1=A_{12}\left[\mathbf{m}_1-\left|\frac{M_2}{M_1}\right|\mathbf{m}_2\right], \tag{10}$$

where the second term represents the interaction of the microwave field with the surface anisotropy field.[10] Clearly, Eq. (10) only affects the dynamic components of the magnetization. We have assumed that the static components of $\mathbf{M}_1$ and $\mathbf{M}_2$ are collinear and parallel to z, since the exchange coupling is ferromagnetic. Henceforth, we will set $K_s=0$.

Except for the front and back surfaces of the structure, there are two of these equations for each interface—one giving the effect of the exchange pinning of the magnetization in the first layer by the magnetization of the second layer, and the other giving the pinning of the second layer through interaction with the first layer. Since the rf magnetization can be related to the rf fields by[9]

$$\mathbf{m}_{n\mu}=-Q_{n\mu}h_{n\mu}, \tag{11}$$

with

$$Q_{n\mu}=\frac{1}{4\pi}\left[1-\frac{i}{2}\delta_0^2k_{n\mu}^2\right], \tag{12}$$

$$\delta_0^2=\frac{c^2}{2\pi\sigma\omega}, \tag{13}$$

we have two more equations relating the fields at each internal interface (only one extra equation is gained from the front and back surfaces). For example, at the interface between layers 1 and 2 ($n=1$ and 2) we have the equation

$$A_1\left[\sum_\mu Q_{1\mu}k_{1\mu}(h_{1\mu}^{+}e^{-ik_{1\mu}d_1}+h_{1\mu}^{-}e^{ik_{1\mu}d_1})\right]$$
$$=A_{12}\left[\sum_\mu Q_{1\mu}(h_{1\mu}^{+}e^{-ik_{1\mu}d_1}+h_{1\mu}^{-}e^{ik_{1\mu}d_1})-\frac{M_2}{M_1}\sum_\mu Q_{2\mu}(h_{2\mu}^{+}e^{-ik_{2\mu}d_1}+h_{2\mu}^{-}e^{ik_{2\mu}d_1})\right], \tag{14}$$

and the other spinning boundary at the common interface is given as

$$A_2\left[\sum_\mu Q_{2\mu}k_{2\mu}(h_{2\mu}^{+}e^{-ik_{2\mu}d_1}+h_{2\mu}^{-}e^{+ik_{2\mu}d_1})\right]$$
$$=A_{12}\left[\sum_\mu Q_{2\mu}(h_{2\mu}^{+}e^{-ik_{2\mu}d_1}+h_{2\mu}^{-}e^{+ik_{2\mu}d_1})-\frac{M_1}{M_2}\sum_\mu Q_{1\mu}(h_{1\mu}^{+}e^{-ik_{1\mu}d_1}+h_{1\mu}^{-}e^{+ik_{1\mu}d_1})\right]. \tag{15}$$

By collecting all of the terms in the internal fields ($h_{1\mu}^{\pm}$) on the right-hand side, we may summarize the boundary condition equations simply as

$$[f]_p=[a]_p[h]_p, \tag{16}$$

where p indicates the particular surface in question. Except for $p=0$ and $p=2N+1$ (the first and last surfaces), $[f]_p$ is a (4×1) column vector matrix in which all the elements are equal to zero; [a] is a (4×8) matrix whose matrix elements are the coefficients multiplying the internal field variables $h_{1\mu}^{\mp}$ and $h_{2\mu}^{\mp}$. For example, $(a_{11})_1=e^{-ik_{1,1}d_1}$. For the other matrix elements the reader is referred to Eqs. (2), (3), (14), and (15). $[h]_1$ is an (8×1) column vector with elements $h_{1,1}^{+},h_{1,1}^{-},h_{1,2}^{+},h_{1,2}^{-},h_{2,1}^{+},h_{2,1}^{-},h_{2,2}^{+},h_{2,2}^{-}$. It is clear that $[a]_0,[a]_{2N+1}$ are (3×8) matrices, since there are three boundary conditions at the first and last surfaces. At either surface there is only one spin boundary condition. Clearly,

$$[f]_0=\begin{bmatrix}h_0\\e_0\\0\end{bmatrix},\quad [f]_{2N+1}=\begin{bmatrix}0\\h_L\\e_L\end{bmatrix}. \tag{17}$$

h_0,e_0, and h_L,e_L are the surface magnetic and electric fields at first and last surfaces, respectively. However, $[h]_0$ and $[h]_{2N+1}$ are still (8×1) column matrices.

We can now put all of the boundary equations into one compact matrix and that is

$$[F]=[A][h], \tag{18}$$

where

$$[F]=\begin{bmatrix}[f]_0\\[f]_1\\\vdots\\[f]_{2N+1}\end{bmatrix},$$

$$[h]=\begin{bmatrix}[h]_0\\\vdots\\[h]_{2N+1}\end{bmatrix},$$

and

$$[A]=\begin{bmatrix}[a]_0 & & & & \\ & [a]_1 & & & \\ & & \ddots & & \\ & & & [a]_{2N} & \\ & & & & [a]_{2N+1}\end{bmatrix} .$$

The $[A]$ matrix is nondiagonal of dimensionality $[4(2N)+6]\times[8(2N+2)]$. The $[F]$ and $[h]$ matrices are column matrices with dimensionalities $[4(2N+6)]\times 1$ and $[8(2N+2)]\times 1$, respectively. $[F]$ may be referred to as the "excitation" matrix, since it contains the incident field amplitudes. $[h]$ contains all internal field amplitudes. Equation (17) is an ordinary matrix equation which occurs often in linear circuit analysis. The matrix $[A]$ may be viewed as the "grand" transfer function of the system.

The object of this calculation is to express e_0 and h_0 in terms of e_L and h_L. For the case of no exchange coupling between layers the relationship between the two sets of surface fields is straightforward.[5] This relationship is simply represented by a 2×2 matrix.[5] From this 2×2 matrix it may be possible[5] to calculate the surface impedance, Z_s, at the two surfaces. For the case of exchange coupling between layers the complication arises from the fact that the $[a]_p$ matrices are nonsquare matrices, since the internal fields in two adjacent layers are now coupled to each other. We show here in this paper that indeed the relationship between the two sets of surface fields is still represented by a 2×2 matrix similar to Ref. 5. Clearly, once this relationship is established we can simply take over all of the algebraic steps used in Ref. 5 to obtain Z_s.

To solve this system of linear equations by matrix inversion is excessively unwieldy. We have adopted a form of Gaussian elimination to eliminate the variables of each layer in turn. Using the four equations at interface 1–2, for example, we can eliminate the variables $h^{\pm}_{1\mu}$ from the three equations for the front surface. We then have three equations for e_0 and h_0 in terms of $h^{\pm}_{2\mu}$. Using the equations for the next interface we can then eliminate $h^{\pm}_{2\mu}$ in terms of $h^{\pm}_{3\mu}$. When we reach the last interface we have six equations in terms of e_0, h_0, h_L, e_L, and $h^{\pm}_{2N+1\mu}$. This allows us to construct[5] a transmission matrix so that given e_0, h_0 we can find e_L, h_L.

We may express the electromagnetic fields at the first surface in terms of fields at the last surface by writing

$$\begin{bmatrix}e_0\\ h_0\end{bmatrix}=\begin{bmatrix}c_{11} & c_{12}\\ c_{21} & c_{22}\end{bmatrix}\begin{bmatrix}e_L\\ h_L\end{bmatrix} , \tag{19}$$

and vice versa

$$\begin{bmatrix}e_L\\ h_L\end{bmatrix}=\begin{bmatrix}b_{11} & b_{12}\\ b_{21} & b_{22}\end{bmatrix}\begin{bmatrix}e_0\\ h_0\end{bmatrix} , \tag{20}$$

where conservation of energy requires that

$$b_{11}=c_{22}/\Delta ,$$
$$b_{12}=-c_{12}/\Delta ,$$
$$b_{21}=-c_{21}/\Delta ,$$
$$b_{22}=c_{11}/\Delta ,$$
$$\Delta=c_{11}c_{22}-c_{12}c_{21} .$$

Furthermore, since the electromagnetic response of the layered structure is reciprocal with respect to the direction of the incident microwave excitation, we also require that

$$\Delta=1 . \tag{21}$$

The matrix elements $c_{11}, c_{12}, \ldots, b_{22}$ are a complicated function of $A_1, A_{12}, g, H, \ldots$. The essential point here is that even for exchange coupling between layers, it may be possible to express the microwave fields at the two outer surfaces by a simple 2×2 matrix with the special constraint that the determinant of the matrix is equal to one. The ratio of the electric to magnetic fields gives the surface impedance of the sample.[5] The real part of the surface impedance[9] is related to the sample FMR absorption.

The major advantage of our approach over previous calculations[6] is that since we successively eliminate variables using the boundary conditions at each interface, we never have to work with a system with more than seven linear equations. Adding additional layers increases the computation time only linearly, rather than by $N!$ as in matrix inversion approaches.

RESULTS

For our calculations we have selected parameters for the two magnetic materials appropriate for iron A and an iron alloy B with parameters as shown in Table I.

Figure 3 illustrates, for a five layer system, the effect of increasing the interlayer interaction A_{12}. With no interlayer interaction, only two peaks are observed in the FMR surface impedance, at exactly the same fields that they would be found in the corresponding single layers. For the excitation of FMR in a single layer the resonance condition is given by Kittel as

$$\frac{\omega}{\gamma}=H-4\pi M , \tag{22}$$

where H is the external magnetic field applied normal to the layer plane, ω is the operating frequency, $\gamma=ge/2mc$, and $4\pi M$ is the saturation magnetization. We have ignored magnetic anisotropy fields in Eq. (22).

TABLE I. Magnetic parameters associated with layers A and B. The operating frequency (f) is 35 GHz, and λ is the Landau-Liftshitz damping parameter.

Layer	$4\pi M$ (kG)	A (10^{-6} erg/cm)	λ (10^7 Hz)	g	σ (10^5 *mho*/cm)
A	21.5	1.91	1.11	2.09	5.8
B	21.0	1.91	1.11	2.09	5.8

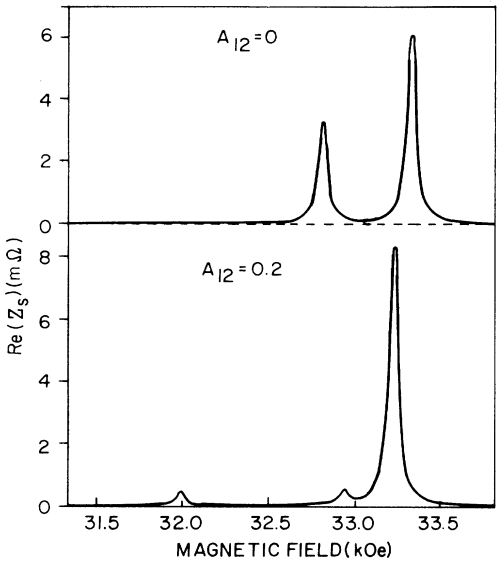

FIG. 3. $\mathrm{Re}(Z_s)$ is plotted as a function of the external magnetic field, H. The operating frequency is 35 GHz and $N=2$, where N is the number of pair layers. The thickness of the iron and iron-alloy layers are 80 Å.

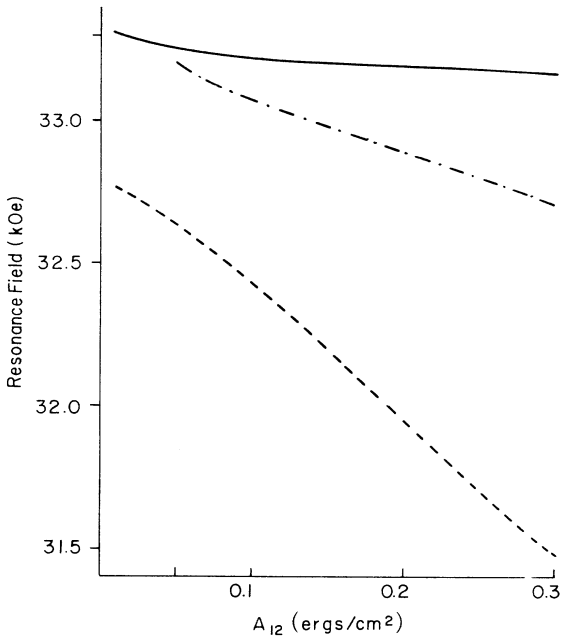

FIG. 4. The field position of the peaks in $\mathrm{Re}(Z_s)$ as a function of the interlayer coupling A_{12}. The frequency is 35 GHz, $N=2$, and the layer thicknesses are 80 Å.

For a single layer of iron $H=33\,461$ Oe assuming $f=35$ GHz, $4\pi M=21.5$ kG, and $g=2.09$, which are parameters appropriate for iron (see Table I). In Table I the above parameters correspond to layer A. For layer B we have assumed $4\pi M=21.0$ kG and all other parameters the same as those of iron. For layer B Eq. (22) gives $H=32\,961$ Oe. Thus, we have chosen layers A and B to be very similar except for their respective values of $4\pi M$. From a material preparation point of view it may be advantageous to prepare layered structures consisting of layers with nearly similar chemical compositions and crystal structures.

As the interlayer interaction is increased to 0.2 erg/cm^2 a satellite peak appears near the high-field (iron) resonance. The splitting between the satellite peak and the main iron peak increases with increasing interaction strength. Simultaneously, the low-field (iron-alloy) peak is pushed to lower fields. The addition of only a single extra peak is understood, since under symmetrical excitation the environment of the two outside iron layers and the two iron-alloy layers is identical. We identify the extra peak as due to the resonance of electrons in the center iron layer.

We can characterize the spectral peaks by three parameters: the FMR field (H_0), the peak height $[\mathrm{Re}(Z_s)]_{\max}$, and the FMR linewidth (ΔH) defined as the full width of the resonance peak at half the maximum height (FWHM). The effect of the interaction parameter A_{12} on the five layer system is summarized in Figs. 4 and 5, which show the variation of the resonance field and peak height as a function of A_{12} (the FMR ΔH is not a strong function of the coupling parameter). The position of the iron-alloy related peak is observed to move rapidly to lower fields and decrease in size as A_{12} is increased. The major iron-related peak shifts only slightly to lower fields and becomes larger. The size of the satellite peak tracks very closely with the size of the iron-alloy peak, but its shift to lower frequencies is not so pronounced. The appearance of the satellite is a dis-

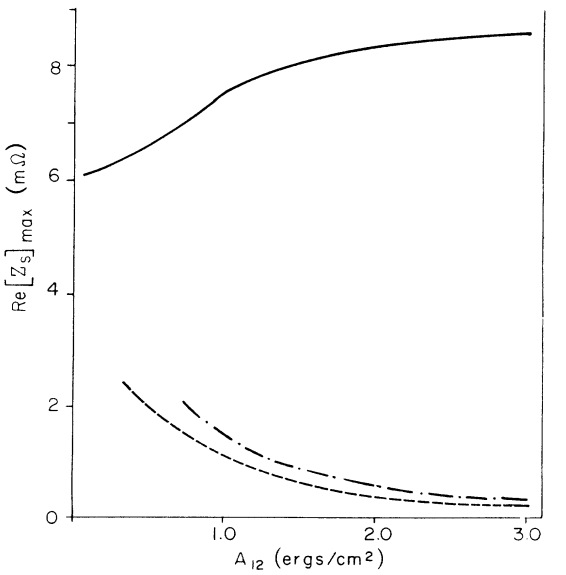

FIG. 5. Peak value of $\mathrm{Re}(Z_s)$ is plotted as a function of A_{12}. The solid, dashed, and dot-dashed lines correspond to the same resonances as in Fig. 4, and all other parameters are as in that figure.

tinctive indication of interlayer exchange coupling, and its field shift is a measure of the strength of the coupling. The close correspondence between the peak heights of the satellite and iron-alloy peaks can distinguish satellite peaks caused by interlayer coupling and features that may be caused by surface anisotropy fields, as discussed below.

As we add layers to the structure the spectra become progressively more complex. Furthermore, the FMR lines become progressively weaker. In order to identify the peak position more exactly we have calculated the derivative of the surface impedance with field (dR/dH). Figure 6 shows the derivative spectra for an 11 layer system. When $A_{12}=0.2$ we see four satellite peaks: two associated with the iron resonance at 33 175 G and two associated with the iron-alloy resonance which has been pushed down to 31 880 G. The dependence of the resonance fields H_0 with the coupling parameter A_{12} is shown in Fig. 7. In this configuration there are three different distinct environments for both the iron and iron-alloy layers. The general rule is that the number of satellite peaks is one less than the number of layer pairs. We illustrate this in Fig. 8, which shows the position and oscillator strength of the peaks in the spectrum as a function of adding layer pairs with the interaction parameter fixed at $A_{12}=0.2$. We note that the satellite peaks enter the spectra between the major peaks, alternately close to the iron peak and the iron-alloy peak.

It is also interesting to study the effect of film thickness on the spectral line shapes. Beginning with five lay-

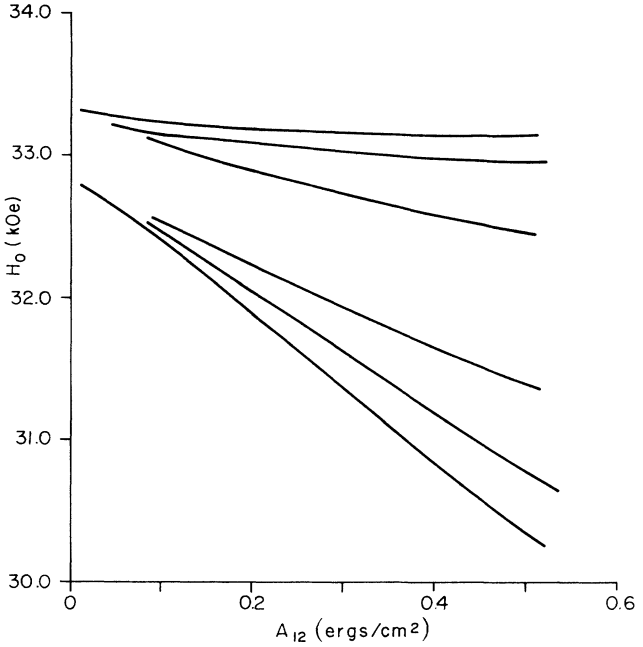

FIG. 7. Dispersion of the FMR resonances as a function of A_{12} in a system with $N=5$. Layer thicknesses are fixed at 80 Å.

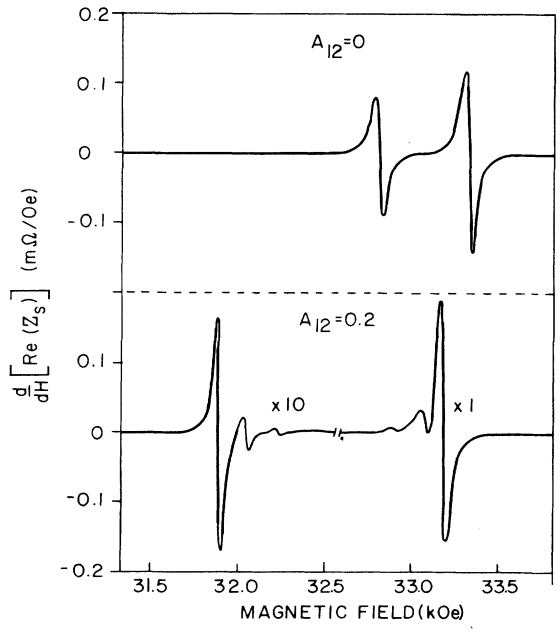

FIG. 6. The derivative of FMR absorption is plotted as a function of H for an 11 layer system ($N=5$). All other parameters are as in Fig. 4.

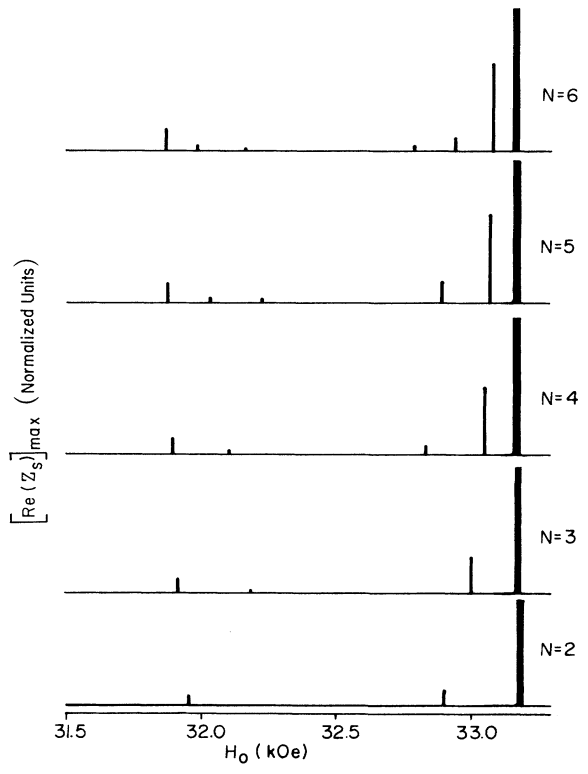

FIG. 8. FMR resonance positions and peak heights are exhibited as a function of H for various N values. $A_{12}=0.2$ and the layer thicknesses are 80 Å. The highest field peak has been reduced in height by a factor of 2 for display purposes.

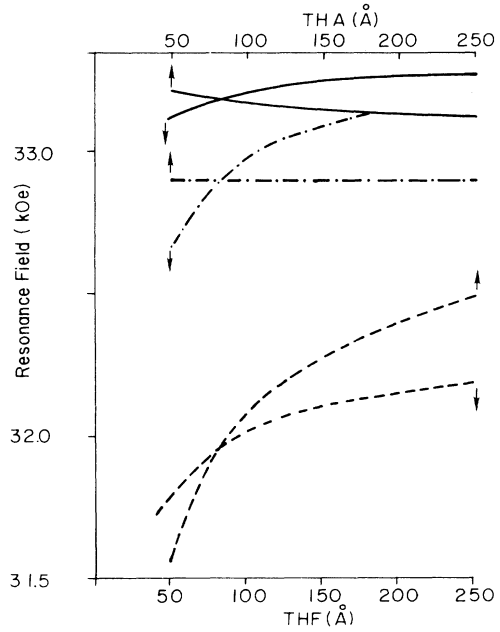

FIG. 9. The FMR resonance fields are plotted as a function of layer thickness of layers A (iron, bottom scale) and B (iron alloy, top scale). $N=2$, $A_{12}=0.2$, and the thickness of the layer not varied is fixed at 80 Å.

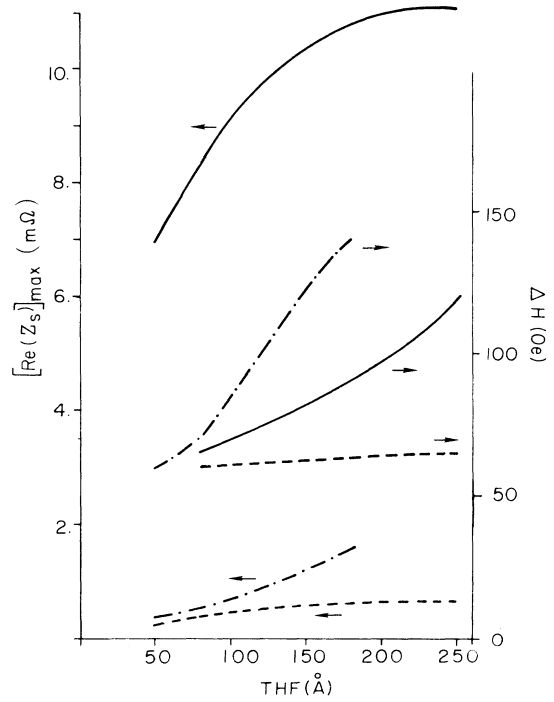

FIG. 10. The peak highs and widths of the FMR resonances as a function of iron-layer thickness for a five-layer system ($N=2$). The iron-alloy layer is 80 Å and $A_{12}=0.2$.

ers with thicknesses of both the iron and iron-alloy layers at 80 Å, Fig. 9 shows how the peak positions shift with the thickness of the iron and iron-alloy layers. It is notable that the position of the satellite peak is a strong function of the iron layer thickness, but is insensitive to the thickness of the iron-alloy layers. The low-field peak associated with resonance in the iron-alloy layer is sensitive to the layer thicknesses of both materials, but the iron-alloy layer thickness has a greater effect.

Figure 10 shows the dependence on the thickness of the iron layers of peak height and width. What is notable here is the strong dependence on the iron-layer thickness of both the peak height and width of the two iron-related lines.

The calculations here were all carried out assuming no surface anisotropy fields [$K_s=0$ in Eq. (9)]. If surface anisotropy fields are taken into account, satellite peaks may result even when $A_{12}=0$. Since surface anisotropy fields are strongly related to interface impurities, it is likely that satellite lines that have been seen thus far in experiments[11] are connected with surface anisotropy. The predictions given for the dependence of the spectra on layer thickness and the number of layers should make it possible to distinguish the effect of interlayer exchange coupling. If the effect of A_{12} can be demonstrated in lattices with mixed materials it will be a unique opportunity to measure exchange constants between different materials.

CONCLUSION

We have calculated the FMR line shape for symmetrical rf excitation of magnetic multilayer structures. The layer components of the multilayer were chosen to be ferromagnetic with their static magnetizations aligned with the external field perpendicular to the layers. The layers were assumed to be uniform with abrupt interfaces and coupled by the exchange potential between atoms of adjoining layers. In the geometry chosen there is no coupling between layers through the magnetic dipole interaction of the rf magnetization. The surface anisotropy fields were set to zero.

We find that the surface impedance shows FMR line shapes that are very sensitive to the exchange coupling between the layers. As the coupling parameter A_{12} is increased, satellite lines are split off the FMR resonance peaks of the component materials. The total number of peaks in the spectra is one more than the number of layer pairs, and the field positions of both the major resonance peaks and the satellites is a strong function of A_{12}. The peak positions, widths, and oscillator strength are also found to depend sensitively on the relative layer thicknesses.

ACKNOWLEDGMENTS

The authors wish to acknowledge the support of the U.S. Office of Naval Research under Contract Nos. N00014-87-K-ONR0041 and N0014-81-K-0252.

[1]R. E. Camley, T. S. Rahman, and D. L. Mills, Phys. Rev. B **27**, 261 (1983); R. E. Camley and M. G. Cottam, *ibid.* **35**, 189 (1987).
[2]J. Barnas, Solid State Commun. **61**, 405 (1987).
[3]Ph. Lambin and F. Herman, Phys. Rev. B **30**, 6903 (1984).
[4]F. Hoffmann, Phys. Status Solidi **41**, 807 (1970).
[5]C. Vittoria, Phys. Rev. B **32**, 1679 (1985).
[6]G. Spronken, A. Friedman, and A. Yelon, Phys. Rev. B **15**, 5141 (1977).
[7]R. M. White and C. Herring, Phys. Rev. B **15**, 5141 (1977).
[8]Y. Yafet (unpublished).
[9]C. Vittoria, J. N. Craig, and G. C. Bailey, Phys. Rev. B **10**, 3945 (1974).
[10]G. T. Rado and J. R. Weertman, J. Phys. Chem. Solids **11**, 315 (1959).
[11]B. L. Ramakrushna, C. H. Lee, Y. Cheng, and M. B. Stearns, J. Appl. Phys. **61**, 4290 (1987).